CrossMark

Multi-scale interactions of equatorial waves associated with tropical cyclogenesis over the western North Pacific

Haikun Zhao[1,2] · Xianan Jiang[2] · Liguang Wu[1] · Philip J. Klotzbach[3]

Abstract

The tropical cyclone (TC)-centric approach developed in previous studies tends to overemphasize the direct impact of tropical waves and underestimates their large-scale modulation of western North Pacific (WNP) tropical cyclogenesis (TCG). To overcome these limitations, this study proposes a new approach based on empirical orthogonal function analyses to re-examine associations of multiple waves, including the Madden–Julian oscillation (MJO), quasi-biweekly oscillation (QBWO), convective equatorial Rossby (ER) waves, and synoptic scale waves (SSWs), with WNP TCG events. There is a close association between WNP TCG events (total of 273 TCs in this study) and SSWs (~ 64%), MJO (~ 68%), QBWO (~ 64%) and ER (~ 65%) waves. These suggest that SSW is critical for many TCG events, and all of these intra-seasonal waves significantly modulate TCG events. A majority of TCs (~ 79%) were found to be related to more than one wave type, indicating an important role for a combination of dynamic and thermodynamic conditions associated with multiple waves in TCG events. Further analyses show that SSW activity is strongly modulated by the MJO and ER waves, while the QBWO has no significant impact on SSWs. During convectively active MJO and ER phases, stronger SSW trains with more distinct southeast-northwestward aligned structures can be found compared to convectively inactive phases. Similar intra-seasonal modulation of the transition from the mixed Rossby-gravity waves from the equatorial central Pacific to the SSW trains over the WNP by the three waves is noted, with such transitions largely favored during convectively active MJO and ER phases.

Keywords Tropical waves · Tropical cyclogenesis · Western North Pacific · Intra-seasonal modulation · Equatorial wave transition

1 Introduction

Multi-scale interactions of tropical waves are generally involved in tropical cyclogenesis (TCG) (Holland 1995; Bister and Emanuel 1997; Landsea et al. 1998; Ritchie and Holland 1999). The impact of the Madden–Julian Oscillation (MJO), convective equatorial Rossby (ER) waves, Kelvin waves, mixed Rossby-gravity (MRG) waves, and synoptic-scale waves (SSW) on TCG has been widely discussed in previous studies (Liebmann et al. 1994; Wheeler et al. 2000; Bessafi and Wheeler 2006; Frank and Roundy 2006; Fu et al. 2007; Klotzbach 2010; Schreck et al. 2011, 2012; Chen and Chou 2014; Klotzbach and Oliver 2015a, b). These studies found that the aforementioned waves contributed to TCG mainly through two ways, namely, by modulating environmental conditions affecting TCG, or by directly providing precursor disturbances for TCG events. The presence of a precursor synoptic-scale disturbance is regarded as a necessary ingredient for TCG (Reed and Recker 1971; Reed et al.

✉ Haikun Zhao
  zhk2004y@gmail.com

1   Key Laboratory of Meteorological Disaster, Ministry of Education(KLME)/Joint International Research Laboratory of Climate and Environment Change(ILCEC)/ Collaborative Innovation Center on Forecast and Evaluation of Meteorological Disaster(CIC-FEMD)/Pacific Typhoon Research Center/Earth System Modeling Center, Nanjing University of Information Science and Technology, Nanjing 210044, China

2   Joint Institute for Regional Earth System Science and Engineering, University of California, Los Angeles, CA, USA

3   Department of Atmospheric Science, Colorado State University, Fort Collins, CO, USA

1977; Yasunari 1979; Nakazawa 1986, 1988; Lau and Lau 1990; Takayabu and Nitta 1993; Dickinson and Molinari 2002; Li and Fu 2006; Li et al. 2006; Li 2006; Tam and Li 2006). Currently, statistical TCG forecast models have been developed and issue forecasts based on the status of these tropical waves (Leroy and Wheeler 2008; Roundy and Schreck 2009). Therefore, in-depth analyses of multi-scale waves from intra-seasonal to synoptic time scales associated with TCG can be helpful for further understanding of the physical processes of TCG and consequent improvements in TCG predictability.

Over the western North Pacific (WNP), one of the most prominent weather phenomena is the frequent occurrence of SSW trains during boreal summer, which are usually aligned in a southwest-northeast direction with a typical wavelength of about 2500–3000 km and a time scale of 3–8 days (Wallace and Chang 1969; Reed and Recker 1971; Lau and Lau 1990; Chang et al. 1996; Maloney and Dickinson 2003; Fu et al. 2007; Zhao et al. 2016a). These SSW trains are generally considered to be an important precursor for WNP TCG (Yasunari 1979; Nakazawa 1986, 1988; Lau and Lau 1990; Zehr 1992; Takayabu and Nitta 1993; Holland 1995; Gray 1998; Sobel and Maloney 2000; Dickinson and Molinari 2002; Li and Fu 2006; Li et al. 2006; Li 2006; Tam and Li 2006). The preference of SSW trains over the WNP basin during boreal summer has a close association with the Asian summer monsoon circulation (Lau and Lau 1990; Takayabu and Nitta 1993; Sobel and Maloney 2000; Dickinson and Molinari 2002; Zhao et al. 2016a), which is further subject to significant modulation by intra-seasonal variability (ISV) modes (Sobel and Maloney 2000; Dickinson and Molinari 2002; Li et al. 2014). In this study, the terminology of "SSW" is the same as the definition of synoptic waves in Zhao et al. (2016a), which is used to specifically represent the southeast-northwest-oriented synoptic wave train over the WNP basin. These SSWs have also been referred to in prior studies as easterly waves, tropical-depression-type disturbances, and synoptic scale disturbances (Riehl 1945; Takayabu and Nitta 1993; Dunkerton and Baldwin 1995; Sobel and Bretherton 1999).

During boreal summer, the 30–70-day MJO and quasi-biweekly oscillation (QBWO) are the two dominant ISV modes over the WNP basin. It is worth noting that the MJO shows eastward propagation near the equator with northwestward propagation over the WNP in both convection and circulation (Hsu et al. 2004; Jiang et al. 2004; Li and Zhou 2013; Zhao et al. 2015a, 2016b). This type of propagation is to be distinguished from the traditional MJO which only has eastward propagation along the equator (Madden and Julian 1971). The QBWO, on the other hand, propagates northwestward along the axis of the East Asian summer monsoon trough with an approximate 10–30-day spectral peak (Chen and Chen 1993; Kikuchi and Wang 2009; Chen

and Sui 2010; Li and Zhou 2013; Zhao et al. 2015a, b). Both dominant ISV modes exert strong modulation on WNP TCG events due to alterations in the environmental conditions (Liebmann et al. 1994; Kim et al. 2008; Camargo et al. 2009; Wang et al. 2009; Huang et al. 2011; Li and Zhou 2013; Zhao et al. 2015a, b). Additionally, the ISV can act as a key seeding disturbance for TCG, which is closely associated with the amplification of high-frequency waves in the ISV convective envelope due to scale contraction and wave accumulation (Nakazawa1986; Sobel and Bretherton 1999; Maloney and Dickinson 2003; Wang et al. 2009; Hsu et al. 2011, Hsu and Li 2011). Moreover, studies have also demonstrated the impact of ER waves on WNP TCG (Roundy and Frank 2004; Frank and Roundy 2006; Molinari et al. 2007; Schreck and Molinari 2009; Zhao and Wu 2018). As indicated in Frank and Roundy (2006), the coherent annual cycle in ER wave activity coincides well with the WNP TC season. Meanwhile, they suggested that ER waves can directly provide a common precursor disturbance and enhance the background convection and low-level cyclonic vorticity, thus impacting TCG.

Most previous studies focused on the influences of equatorial waves on TCG events (Dickinson and Molinari 2002; Schreck and Molinari 2009; Frank and Roundy 2006; Bessafi and Wheeler 2006; Schreck et al. 2011, 2012; Chen and Chou 2014; Wu and Takahashi 2017). Recently, a TC-centric approach was used to investigate the fraction of the specific WNP TCG events associated with various wave types (Schreck et al. 2011; Chen and Chou 2014). In their studies, each TCG event was attributed to a wave type when the filtered rainfall anomaly exceeded a threshold at the TCG location and time. A constant threshold was used in Schreck et al. (2011) to assess the respective direct association of TCG with each of the five wave types including the MJO, Kelvin waves, ER, MRG, and SSW, and relatively consistent results are found for a range of thresholds from 2 to 4 mm day^{-1}. In contrast, varying thresholds were adopted in Chen and Chou (2014) for each of the three wave types investigated in their study (MJO, ER and SSW). They used different thresholds in consideration of varying standard deviations and geographic distributions of different wave types. Specifically, one TC genesis event is considered to be attributed to one given wave type when the mean wave-filtered anomaly within the $4° \times 4°$ domain centered in TC genesis locations is more than one-half of the standard deviation of the corresponding wave type. However, some drawbacks are noted in these two studies. First, only the eastward propagating MJO mode was considered in these two studies, which could considerably underestimate the role of the northwestward propagating boreal summer MJO mode in WNP TCG (Li and Zhou 2013; Zhao et al. 2015a, b; Hsu et al. 2004). Second, the direct role of the QBWO in WNP TCG cases was not discussed in these two studies, although the strong

impact of the QBWO on WNP TCG events has been widely documented (Wang et al. 2009; Li and Zhou 2013; Zhao et al. 2015a, 2016b). The plausible and complex relationship between ER waves and QBWO mode may be one of the main reasons. For example, ER waves can contribute to the origin of the QBWO mode (Chen and Sui 2010). However, studies suggested that the ER wave was distinct from the QBWO mode over the WNP basin in terms of spatial and temporal evolution patterns and thus had a significantly different impact on WNP TCG events (Zhao and Wu 2018). In addition, wave-related filtered anomalies in each wavenumber-frequency band were adopted in these two studies, which may contain unrelated rainfall activity for each wave. Lastly, the TC-centric approach focused on the direct influences of equatorial waves on TC genesis and consequently does not account for the large-scale dynamical or indirect influences of equatorial waves on TCG events. Although studies have suggested that the enhancement of convection is possibly one of the primary mechanisms for equatorial waves to foster TCG (Liebmann et al. 1994; Dickinson and Molinari 2002; Frank and Roundy 2006), the indirect impact of large-scale modulation on TCG cases is likely significant.

Motivated by the considerations mentioned above, the association of multiple waves with WNP TCG events is re-examined here. A new approach is adopted in this study to investigate the direct association of multiple waves with WNP TCG events. The three wave types discussed in Chen and Chou (2014) are also considered here in addition to the QBWO. As suggested by previous studies (Frank and Roundy 2006; Chen and Chou 2014; Wu and Takahashi 2007), the classic Kelvin wave structure is hard to discern in the winds using a Kelvin wave-band composite relative to TCG locations. Moreover, Kelvin waves over the WNP exhibit no significant annual cycle, and therefore do not demonstrate a coherent phase relationship with the TC season over the WNP basin. Due to the unclear relationship between TCG cases and Kelvin waves, the attribution of Kelvin waves to WNP TCG events is not discussed further in this study. Therefore, the results outlined in Chen and Chou (2014) are referred to as the main reference for assessing the performance of our proposed approach.

Additionally, some studies illustrated that MRG waves can transition to SSWs and grow rapidly when the MGR waves propagate westward along the equator and encounter a favorable tropical basic state. This transition can be modulated by climate variations such as the MJO (Aiyyer and Molinari 2003; Kiladis et al. 2009; Chen and Sui 2010). In this study, the transition of MRG waves to SSW trains under different intra-seasonal large-scale conditions is also examined.

The rest of this study is arranged as follows. Section 2 describes the datasets used. The proposed approach for identifying multiple wave types associated with WNP TCG events is also introduced in this section. Section 3 analyzes the number of WNP TCG events attributed to the various wave types and combination of wave types as well as the associated wave characteristics related to TCG events for each of the different categories. Modulation of the three intra-seasonal wave types (i.e., MJO, QBWO and ER wave) on SSW activity over the WNP is investigated in Sect. 4. Similar analyses of the modulation of the transition of the westward MRG wave to the northwestward SSW trains by these three waves are explored in Sect. 5. A summary is given in Sect. 6.

2 Datasets and methodology

2.1 Observational datasets

Rainfall observations during 1998–2012 from the Tropical Rainfall Measuring Mission (TRMM product 3B42, version V7; Huffman et al. 2007) precipitation dataset are used to identify the leading MJO, QBWO, MRG waves and SSW. TRMM 3B42 is a global precipitation product based on multi-satellite and rain gauge analyses. It provides precipitation estimates with a 0.25° spatial resolution extending from 50°S to 50°N at a 3-hourly interval. Daily sea surface temperature (SST) and atmospheric fields including temperature, specific and relative humidity, winds, and pressure vertical velocity are derived from the European Center for Medium Range Weather Forecasting (ECMWF) ERA-interim reanalysis (Dee et al. 2011) with a 1.5° horizontal resolution.

TC data over the WNP basin are obtained from the Joint Typhoon Warning Center (JTWC), including positions and intensities of tropical storms and typhoons at 6-hourly intervals. Only TCs with a maximum sustained wind greater than 17.3 ms^{-1} (e.g., named storms) are considered in this study. The peak TC season is defined to be May to October, and we examined the period from 1998 to 2012 for this analysis. There were a total of 273 WNP TCG events during the peak TC season in these years.

2.2 Methodology

To restrict our consideration to the region of interest and to reduce the dimensionality of the data required for representing each wave, an empirical orthogonal function (EOF) analysis of the filtered fields is performed over the specific domain. This type of EOF analysis was also used in several previous studies (Wheeler and Hendon 2004; Bessafi and Wheeler 2006; Kiladis et al. 2009; Jiang et al. 2012; Li and Zhou 2013; Zhao et al. 2015a, b). The EOF domain [0–30°N, 100°–180°E] is selected for extracting the MJO, QBWO, ER and SSW types over the WNP basin. In terms of

the MRG wave gyres centered on the equator over the central Pacific and their transition to off-equatorial gyres which then propagate northwestward toward the Philippines region, a domain of [30°S–30°N, 135°E–140°W] is used for the EOF analysis of 2–10-day westward filtered rainfall anomalies to extract the westward MRG waves.

The first two leading EOFs of each wave type are chosen to demonstrate a quadrature relationship that indicates wave propagation and structure in the region, similar to what has been done in previous studies (Wheeler and Hendon 2004; Bessafi and Wheeler 2006; Jiang et al. 2012; Li and Zhou 2013; Zhao et al. 2015a, b, 2016a, b, 2018; Zhao and Wu 2018). To extract the two leading ISV modes over the WNP basin, e.g., the MJO and QBWO, an EOF analysis is applied to daily 10–90-day bandpass-filtered TRMM rainfall anomalies during 1998–2012. The first two leading pairs of EOF modes can be well separated from each other using the formula from North et al. (1982). The MJO (QBWO) mode over the WNP can be identified by the first (second) leading pair of EOF modes as shown in Fig. 1a–d, respectively. Based on the evolution of their respective first EOF modes, a prominent north-northeastward (northwestward) propagation can be found (figure not shown). Spectral analyses of the corresponding principal components (PCs) further suggest a peak period of about 40 days and 16 days for the first and second leading modes, respectively (figures not shown). The spatio-temporal characteristics of the first two modes are consistent with previous studies (Yasunari 1979; Wang and Rui 1990; Chen and Chen 1993, Hsu et al. 2004; Jiang et al. 2004; Chen and Sui 2010; Li and Zhou 2013; Zhao et al. 2015a, b). Overall, the first two leading EOF modes of observed daily rainfall anomalies capture well the dominant boreal summer MJO mode and QBWO mode over the WNP basin.

Similarly, the ER-filtered rainfall anomalies are used for EOF analyses to extract the ER wave. The ER-filtered rainfall anomalies are computed based upon the ER band with a period of 10–48 days and wavenumbers of -10 to -1 as adopted in previous studies (Schreck et al. 2011; Chen and Chou 2014; Zhao and Wu 2018). The propagating features of the ER wave can be well represented by the two leading modes of ER-filtered rainfall anomalies (Fig. 1e, f). Studies suggested distinct features between QBWO and ER waves mainly in term of their spatial patterns and impacts on weather events (e.g.,TCG) (Wheeler et al. 2000; Yang et al. 2007; Zhao et al. 2015a, b; Zhao and Wu 2018), although there is certainly a close relationship between QBWO and ER waves (Chen and Chen 1993; Numaguti 1995; Kikuchi and Wang 2009; Chen and Sui 2010). For example, in comparison with the significant northwestward propagation of the QBWO as shown in Fig. 1c, d, the ER wave pattern exhibits more zonal extension than meridional, consistent with previous studies (Wheeler et al. 2000; Yang et al.

2007; Zhao and Wu 2018). Additionally, there is no overlap between the MJO mode and ER mode in the wavenumber-frequency space because MJO mode have eastward (positive) wavenumbers and ER mode have westward (negative) wavenumbers.

Following previous studies (Kiladis et al. 2009; Zhao et al. 2016a), an EOF analysis of the 2–10-day westward filtered rainfall anomalies is used for extracting the leading SSW mode (Fig. 1g, h). Represented by the two leading EOF modes, the SSW is characterized by alternating positive and negative rainfall anomalies center aligned in a southeast to northwest direction with a typical wavelength of about 2500–3000 km and a peak period of 6 days, in agreement with previous studies (Lau and Lau 1990; Maloney and Dickinson 2003; Li 2006; Tam and Li 2006; Fu et al. 2007; Zhao et al. 2016a).

Considering the rainfall associated with TCs contribution to the wave variance (Hsu et al. 2008; Schreck et al. 2011, 2012; Chen and Chou 2014), we conducted similar EOF analyses of each wave type during these non-TC days (1468 days) from 1998 to 2012. It was found that these wave types identified by the first two leading EOF modes are similar to those based on EOF analysis during the 15 full summers (figure not shown). These indicated that each wave type over the WNP basin revealed by the EOF analyses represent two intrinsic convective variability modes.

3 TC categorization and wave characteristics

3.1 Definition of attribution

To derive a potentially more accurate estimate of the role of each wave in modulating WNP TCG over the TC-centric approach employed in previous studies (Schreck et al. 2011; Chen and Chou 2014), an objective definition of attribution is proposed in this study by taking into account the large-scale modulation of these wave types. In this proposed approach, a TCG case is attributed to one given wave based upon two criteria. The first is that the EOF-based reconstructed rainfall anomalies for one given wave type in the $5° \times 5°$ box with the center of a TCG location at the TCG time exceeds zero. The EOF-based reconstructed rainfall anomaly for one given wave is computed as $P_{rec} = PC1 \times EOF1 \times PC2 \times EOF2$. Our examination suggested that the $5° \times 5°$ box for computing P_{rec} is a reasonable selection to represent the large-scale environment associated with these wave types. It was additionally found that the larger domain for computing P_{rec} has a slight impact on the attribution of TCG events to each given wave type. The second criteria is that the wave amplitude of one given wave type exceeds 0.5 at the TCG time. The principal components (PCs) of the first two leading
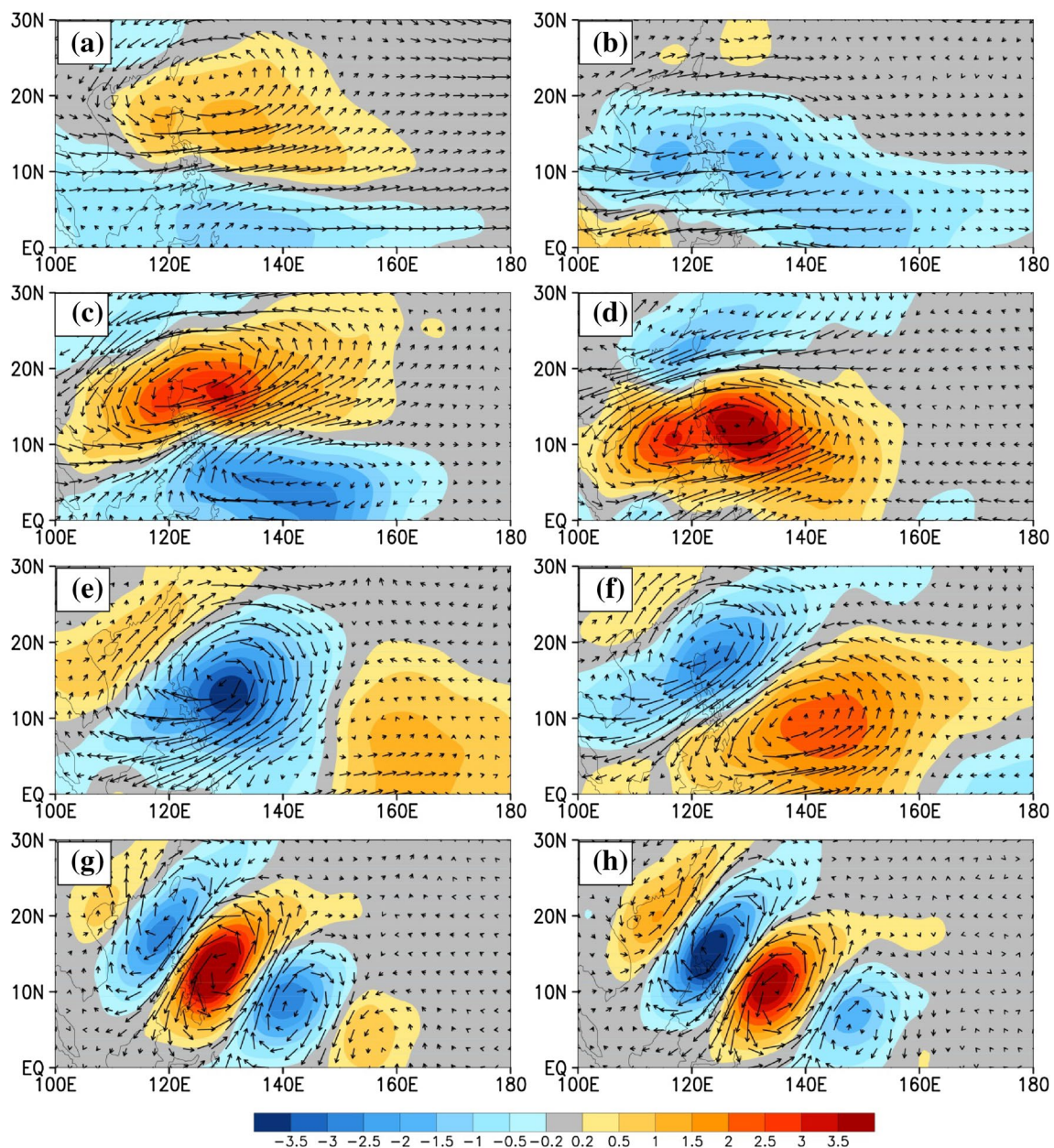
Fig. 1 Principal components (PCs) of the first two leading EOF modes regressed onto corresponding filtered rainfall anomalies (shading) and 850-hPa winds (vectors) for the western North Pacific (WNP) boreal summer Madden–Julian oscillation (MJO) shown in (**a, b**), quasi-biweekly oscillation (QBWO) shown in (**c, d**), convective equatorial Rossby (ER) wave shown in (**e, h**) and synoptic scale wave (SSW) shown in (**g, h**)

EOF modes are used to identify the daily wave amplitude i.e., Sqrt(PC1*PC1 + PC2*PC2) and phases (ranging from 1 to 8), following Wheeler and Hendon (2004). The 0.5 threshold of the wave amplitude is determined after a series of sensitivity tests, which is mainly based upon the previously-documented percentage of TC events associated with SSW over the WNP basin (Ritchie and Holland 1999; Fu et al. 2007; Schreck et al. 2011; Chen and Chou 2014). When using different threshold values, similar results can be found except for different percentages associated with all wave types and the intensity of each wave type. Although the percentage of TCs attributed to each wave type is sensitive to the threshold selection, the relative importance of each wave type is consistent for a a variety of thresholds (figure not shown).
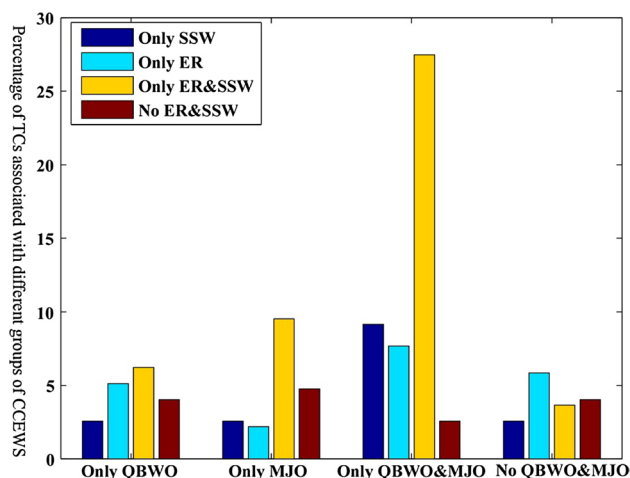
Fig. 2 Percentages of tropical cyclogenesis (TCG) events over the WNP basin divided into sixteen categories. Note that no TCG cases overlap within the different categories

3.2 TC categorization

As shown in Fig. 2, the 273 WNP TCG events from May to October during the period of 1998–2012 are classified into 16 categories. There are four categories in which TCG cases are attributed to a single wave type at the time of TCG. The corresponding percentage of TCG events in these four categories indicates the respective direct linkage of the WNP TCG events with each one of these four wave types. They are respectively displayed in Fig. 2 with "only QBWO and No ER&SSW", "only MJO and No ER&SSW", "only ER and No QBWO&MJO", and "only SSW and No QBWO&MJO". TCG events associated with two wave types can be divided into six categories. The corresponding percentages are shown in Fig. 2 with "only QBWO and SSW", "only QBWO and ER", "only MJO and SSW", "only MJO and ER", "only QBWO and MJO", and only ER and SSW, respectively. Also, the TCG events related to three wave types can be divided into four categories, which are represented as "only QBWO and only ER&SSW", "only MJO and only ER&SSW", "only MJO&QBWO and only SSW", and "only MJO&QBWO and only ER". The remaining two categories are represented by "only MJO&QBWO and only ER&SSW" (hereafter denoted as "all" category) and "No QBWO&MJO and No ER&SSW" (hereafter denoted as "none" category), which respectively indicate all and none of the four wave types contributing to WNP TCG events. According to these 16 classifications, all 273 TCG events can be partitioned into individual groups without overlapping. Thus, there are no TC cases that overlap within the different categories, and consequently they sum to 100%.

3.3 Statistics of TCG events associated with different categories

In this study, the percentage of TCG events with no impact of the four wave types (i.e., none category) is relatively low, accounting for only 4.3% of all TCG cases (Fig. 2), similar to the 5.6% of all TCG cases without any contribution from multiple waves noted in Chen and Chou (2014). Although some studies suggested that these TCG events could be associated with the impact of upper-level trough interaction (Sadler 1976), tropical transition (Davis and Bosart 2001), or localized mesoscale convective systems within the monsoon trough (Ritchie and Holland 1999), no explicit mechanism has currently been given for these WNP TCs that form in the absence of an equatorial wave precursor disturbance. Consequently, this formation type needs further study.

Also shown in Fig. 2 are TCG events that are attributed to a single wave type. They account for 47 of the 273 cases (17.2%) investigated here. TCG events related to only ER waves make up the largest single wave type (5.9%), similar to results from Chen and Chou (2014). The number of TCG events associated with only SSW is the lowest, accounting for about 2.5% of all TC cases. To a certain extent, this implies that fewer TCs are associated with SSW trains by themselves. This may be due to weak SSW wave amplitude with lack of modulation by other large-scale waves (Lau and Lau 1992; Sobel and Bretheron 1999; Sobel and Maloney 2000). TCG events associated with only a single MJO (i.e., 4.8%) and only a single QBWO (i.e., 4.0%) are shown in Fig. 2, indicating that these two dominant ISV modes can also directly provide precursor disturbances for WNP TCG. As suggested by previous studies (Nakazawa 1986; Maloney and Dickinson 2003), ISV can act as a key ingredient for establishing a convective envelope, during which the amplification of high-frequency waves is supported by scale contraction and wave accumulation. Note that discrepancies in the percentages of TCG events associated with only one given wave type can be found between results from Chen and Chou (2014) and this study. For example, the percentage of TCs associated with only ER waves in the present study (5.9%) is much lower than the 12% documented in Chen and Chou (2014). Both the percentage of TCG events associated with only the MJO (4.8%) and only SSW (2.5%) are lower than those in Chen and Chou (2014). After close examination, it is found that these differences are largely due to differences in identification of tropical waves and different study periods. Chen and Chou (2014) used filtered anomalies in each wavenumber-frequency band, which may contain unrelated rainfall activity for each wave. In our approach, the anomalies associated with individual wave patterns by EOF are more focused.

Additionally, the ER wave anomaly defined by Chen and Chou (2014) could include some QBWO signal. The attribution of QBWO on TCG events was not considered in their study but has been examined in this study. TCG events studied in Chen and Chou (2014) were also slightly different from what were examined here due to different study periods. Our study period is from May to October for the period of 1998–2012 with 273 TCG events, while Chen and Chou (2014) examined from May to November during the period of 1998–2010 with 213 TCG cases.

Approximately 78.5% of the total of 273 WNP TCG cases had contributions from more than one wave type. Nearly 2/3 of the TCG events (i.e., 66%) had contributions from the MJO with or without other wave interaction. Similarly, about 65% (68%) of the WNP TCG cases were found to be associated with the QBWO (ER) wave. The relatively large contributions of these three intra-seasonal wave types to WNP TCG events confirms the strong modulation of WNP TCG events by these intra-seasonal wave types that has been documented in previous studies (Frank and Roundy 2006; Huang et al. 2011; Li and Zhou 2013; Zhao and Yoshida 2015; Zhao et al. 2015, 2016; Zhao and Wu 2017). Additional analysis shows that a larger percentage of TCG events associated with the two dominant ISV modes can be found than with individual ISV modes (Fig. 2), agreeing well with findings from previous studies that more TCG cases occur during periods when both the simultaneous MJO and QBWO phases were convectively active (Gao et al. 2011; Li and Zhou 2013; Zhao et al. 2015).

A majority of WNP TCG events (about 64% of the total of 273 TCs) are associated with SSWs including contributions from SSWs with or without other wave types, confirming results of previous studies that SSW trains serve as a major seed for WNP TCG (Lau and Lau 1990; Ritchie and Holland 1999; Frank and Roundy 2006; Li and Fu 2006; Li 2006; Fu et al. 2007; Schreck et al. 2011, 2012). By analyzing datasets from both high-resolution satellite and NECP/NCAR Reanalysis, Fu et al. (2007) identified that about 50% of the total of the 34 WNP TCG events that occurred in 2000–2001 were associated with SSW trains. More recently, Chen and Chou (2014) suggested that about 60% of the total of 214 WNP TCG events during 1998–2010 were closely related to SSW trains over the WNP basin. These studies illustrated that SSW trains play an important role in triggering WNP TCG, although some differences in the percentage of TCs related to SSW trains can be found in these studies (Ritchie and Holland 1999; Fu et al. 2007; Chen and Chou 2014). Further comparisons indicate that these slight differences are mainly due to different approaches for identifying TC events with SSW trains as well as the different time periods examined in each study.

3.4 Wave characteristic associated with the WNP TCG

Evidence of the wave-preferred phase relationships to WNP TCG is provided by displaying the composite 850 hPa winds and TRMM rainfall anomalies of the four wave types at the time and location of TCG during the four specific categories. During each one of the four categories, all TCs are defined to be from one given wave type with or without the combination of other waves. For brevity, these four categories are referred to as the MJO-associated, QBWO-associated, ER-associated and SSW-associated categories. Our calculations suggest that 74, 69 and 69% of TCs during the SSW-associated category, respectively, are found to be related to the MJO-associated, QBWO-associated, and ER-associated categories, These imply a close association between SSW activity and these intra-seasonal wave types, as well as the important role of multi-scale interaction of these multiple waves on WNP TCG.

Composites of EOF-based reconstructed rainfall and 850-hPa wind anomalies relative to the TCG location and time are shown during the MJO-associated (Fig. 3a), QBWO-associated (Fig. 3b), ER-associated (Fig. 3c), and SSW-associated (Fig. 3d) categories, respectively. Distinct wave characteristics can be found for each category. During the MJO-associated category, the mean TCG location is situated within the center of MJO-enhanced convection to the north of a strong and persistent westerly surge (Fig. 3a). A clear northwestward alignment in convection and circulation can be observed for the QBWO-associated category, in which TCs are likely to form in the region of maximum low-level cyclonic vorticity and convection (Fig. 3b). These wave characteristics during the MJO-associated and QBWO-associated categories compare well with previous studies (Kim et al. 2008; Kikuchi and Wang 2009; Huang et al. 2011; Li and Zhou 2013; Zhao et al. 2015a, b, 2016b).

As shown in Fig. 3c, a classic ER wave pattern in terms of the EOF-based reconstructed rainfall and 850-hPa wind anomalies can be readily seen during the ER-associated category. The characteristics of the ER-associated category shown in Fig. 3c compare well with what is found in previous studies (Wheeler et al. 2000; Frank and Roundy 2006; Yang et al. 2007; Chen and Sui 2010; Chen and Chou 2014; Zhao and Wu 2017). The ER wave propagates more zonally than meridionally. The positive rainfall anomaly center is located to the east of a cyclonic gyre. Additionally, the mean TCG location is situated on the southeastern side of the strong cyclonic gyre. Figure 3d shows the composite wave structure related to the SSW-associated category, which exhibits a clear orientation in the southwest-northeast
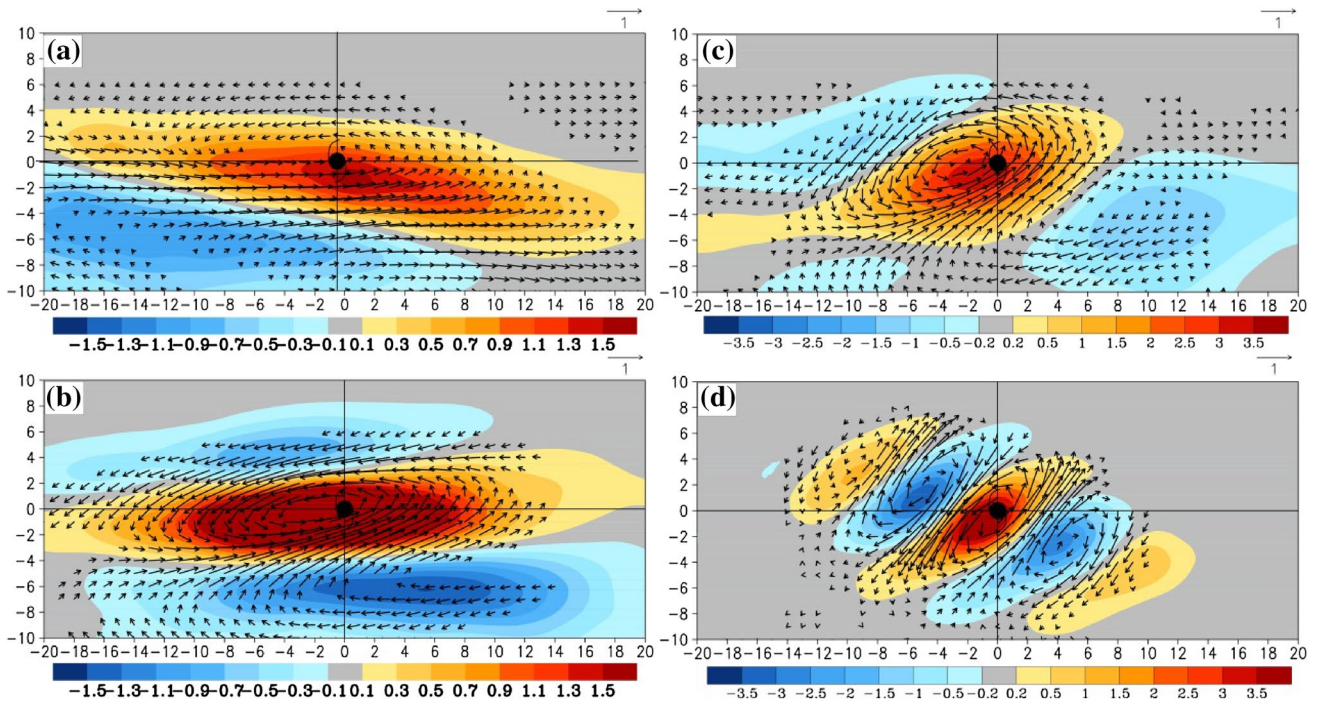
Fig. 3 Composites of the filtered anomalies of 850 hPa-winds and TRMM rainfall relative to the TCG location and time for the MJO-associated (**a**), QBWO-associated (**b**), ER-associated (**c**), and SSW-

associated categories (**d**). Only values of 850 hPa wind anomalies exceeding the 95% confidence level have been plotted
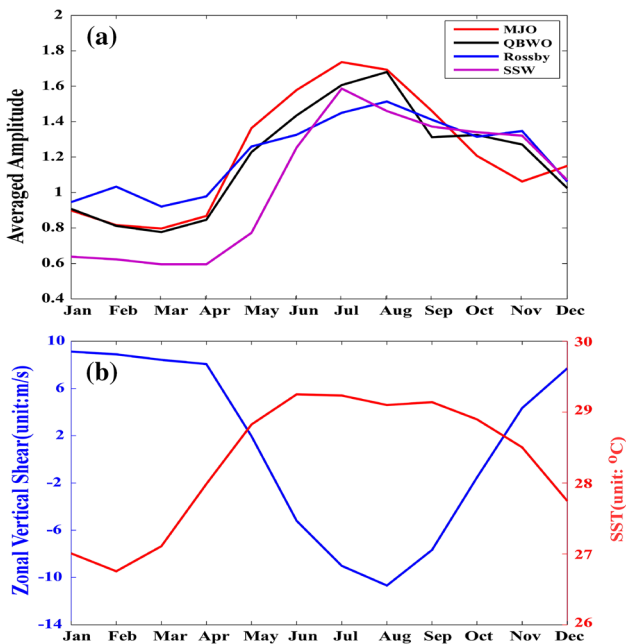

Fig. 4 **a** Seasonal cycle of amplitude for the MJO, QBWO, ER wave and SSW, and **b** seasonal cycle of sea surface temperature (SST) in red and zonal wind shear (U850–U200) in blue over the WNP basin

direction and a typical wavelength of about 2500 km, similar to what was found in prior studies (Lau and Lau 1990; Dickinson and Molinari 2002; Li 2006; Fu et al. 2007).

4 Intra-seasonal modulations on SSW wave activity

A consistent seasonal cycle of amplitudes can be clearly observed among all four wave types (Fig. 4a). Generally, wave amplitudes significantly increase in June and then remain at high levels until October, agreeing well with seasonal variations of WNP TC frequency (figure not shown). Similar results were found in Frank and Roundy (2006). This result suggests that there may be a close association between these four wave types and TCG events over the WNP. However, the consistent season cycle appears to be extraordinarily different with the previous studies (Wu and Takahashi 2017; Frank and Round 2006). There are three main possible reasons for this inconsistence. One reason is that the direct impacts of tropical different waves on TCG over the WNP basin were examined. For example, the impact of Kelvin waves on TC genesis over the WNP basin was discussed in

these previous studies, while the role of Kelvin wave is not examined in this study. In contrast, the impact of QBWO mode on the WNP TCG events was investigated in this study, while it was not considered in previous studies. Another is a different method of extraction of the MJO mode. Only the eastward propagating MJO mode was considered in previous studies, which could largely underestimate the role of the northwestward propagating boreal summer MJO mode on WNP TCG (Hsu et al. 2004; Li and Zhou 2013; Zhao et al. 2015a, b). In this study, EOF analysis was used to extract the MJO mode over the boreal summer. This approach captures well the northwestward propagation of the MJO mode over the WNP basin (Zhao et al. 2015a, b). Moreover, a new decomposition of equatorial wave types associated with TCG events was developed in this study, different from the TC-centric approach used in previous studies.

Previous studies have identified some dynamic and thermodynamic environmental factors (e.g., SST, vertical wind shear, and low-level vorticity) responsible for rapid SSW development which thus may affect TCG (Gray 1979; Li and Wang 1994; Wang and Xie 1996; Kuo et al. 2001; Maloney and Dickinson 2003; Li 2006; Zhao et al. 2017). By comparing Fig. 4a, b, the amplitudes of all four of these waves with respect to the seasonal cycle exhibit highly positive correlations with SST and highly negative correlations with vertical wind shear over the main development region for WNP TCs, consistent with previous studies (Li and Wang 1994; Wang and Xie 1997; Li 2006). During the peak TC season, warmer SSTs can be found over the WNP basin, coinciding with vigorous SSW activity over the WNP basin. This may be due to the increase of moist static energy accompanied with these warmer SSTs and greater oceanic heat content, which thus make a more conditionally unstable stratification in this region (Li and Wang 1994). Meanwhile, easterly wind shear prevails over the WNP basin during May–October, and westerly wind shear is observed in other months (Fig. 4b), corresponding to more vigorous SSW activity during the boreal summer. As suggested by Li (2006), easterly shear favors much faster growth of SSW activity than an environment with westerly shear, based on the dynamical framework of convection-frictional convergence feedback. This result, however, seems to go against our recent study based upon multi-model simulations (Zhao et al. 2016a) that showed that vertical wind shear was not closely associated with simulations of SSWs. Moreover, simulating tropical equatorial waves remains a great challenge (Serra et al. 2014). Mechanisms responsible for tropical wave activity are still not unclear and require further study.

On intra-seasonal time scales, large-scale factors such as SST, moisture, low-level vorticity, and vertical wind shear can be strongly modulated by the MJO, QBWO and ER
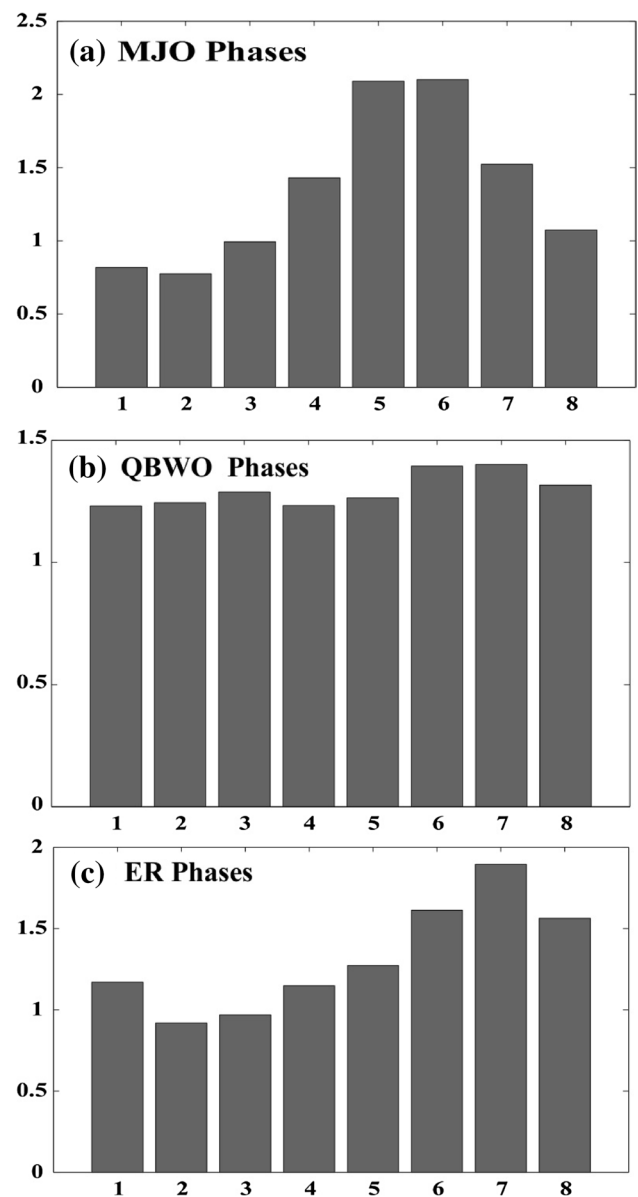

Fig. 5 SSW amplitudes during **a** MJO phases, **b** QBWO phases, and **c** ER phases, respectively

waves and thus further affect SSW activity. Their respective modulation of WNP SSW activity is first examined by displaying the composite SSW amplitude during a life cycle of the MJO (Fig. 5a), QBWO (Fig. 5b) and ER wave (Fig. 5c) respectively. Remarkable changes in SSW amplitude along with the evolution of the MJO and ER wave types can be found, while no substantial difference in SSW amplitude occurs during any of the QBWO phases. During the enhanced convective period associated with the MJO from phases 4–6, a stronger SSW amplitude is readily seen
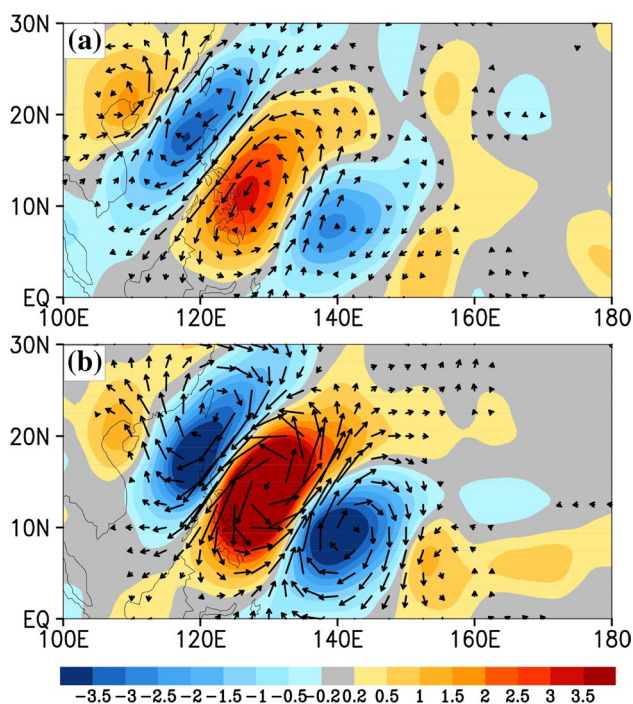
Fig. 6 Regression patterns of 2–10-day westward-filtered rainfall anomalies and 850 hPa wind anomalies onto the principal components (PCs) of the first SSW EOF mode during **a** inactive MJO phases 1–2 and **b** active MJO phases 5–6. Only values of 850 hPa wind anomalies exceeding the 95% confidence level have been plotted
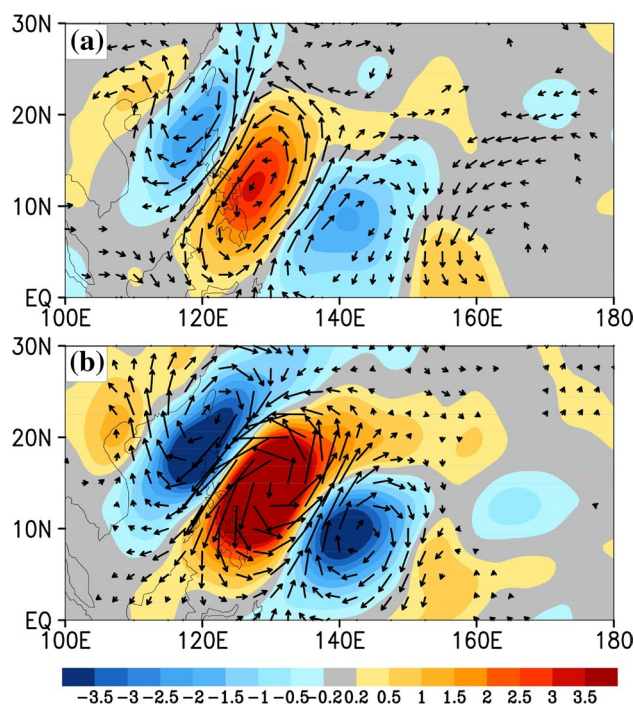
Fig. 7 Regression patterns of 2–10-day westward-filtered rainfall anomalies and 850 hPa wind anomalies onto the principal components (PCs) of the first leading SSW EOF mode during **a** inactive ER phases 2–3, and **b** active ER phases 6–7. Only values of 850 hPa wind anomalies exceeding the 95% confidence level have been plotted

compared to that during the suppressed period from phases 1–3 and phase 8 (Fig. 5a). This is further confirmed by the regression patterns of 2–10-day westward-filtered rainfall anomalies and 850-hPa winds anomalies onto PCs of the first leading SSW EOF mode (i.e., PC1) during the active MJO phases 5–6 (Fig. 6a) and during the inactive MJO phases 1–2 (Fig. 6b) respectively. Regression patterns show that stronger SSW trains with a clearer southeast-northwest direction can be found during active MJO phases compared to that during inactive MJO phases. Similar to the role of the MJO on SSW activity, a more prominent SSW train aligned in a southeast-northwest direction can be observed during the convectively active ER phases 6–7 compared to that during the convectively suppressed ER phases 2–3 (Fig. 7).

5 Intra-seasonal modulations of the transition of MRG waves to SSWs

Previous studies suggested that SSW precursor perturbations for the WNP TCG commonly originate from equatorial MRG waves that propagate westward from the central to the western Pacific into a region characterized by a monsoon

environment (Hartmann and Maloney 2001; Dickinson and Molinari 2002; Aiyyer and Molinari 2003; Zhou and Wang 2007; Chen and Huang 2009; Chen and Sui 2010). They suggested that MJO-forced low-level convergence favors this transition from MRG to SSWs by wave accumulation. MRG wave propagation into the East Asian monsoon convergence zone could amplify through a reduction in scale and wave energy accumulation processes (Holland 1995; Sobel and Bretherton 1999; Kuo et al. 2001) and thus modify its evolution into the SSW trains over the WNP basin. As suggested by previous studies (Kim et al. 2008; Huang et al. 2009; Chen and Sui 2010; Li and Zhou 2013; Zhao et al. 2015a, b, 2016a, b; Zhao and Wu 2018), the three intra-seasonal wave types (i.e., MJO, QBWO and ER waves) can significantly modulate the monsoonal circulation over the WNP basin, but how the three intra-seasonal waves affect the transition of MRG waves to SSWs requires further investigation. In this section, we mainly focus on their modulation of the transition of MRG waves to SSWs over the WNP basin. As introduced in Section 2b, the MRG wave is also identified by the EOF approach. Similarly, a pair in approximate quadrature with westward propagation for the two first leading modes (Fig. 8a, b) is displayed. Equatorial antisymmetric anomalies
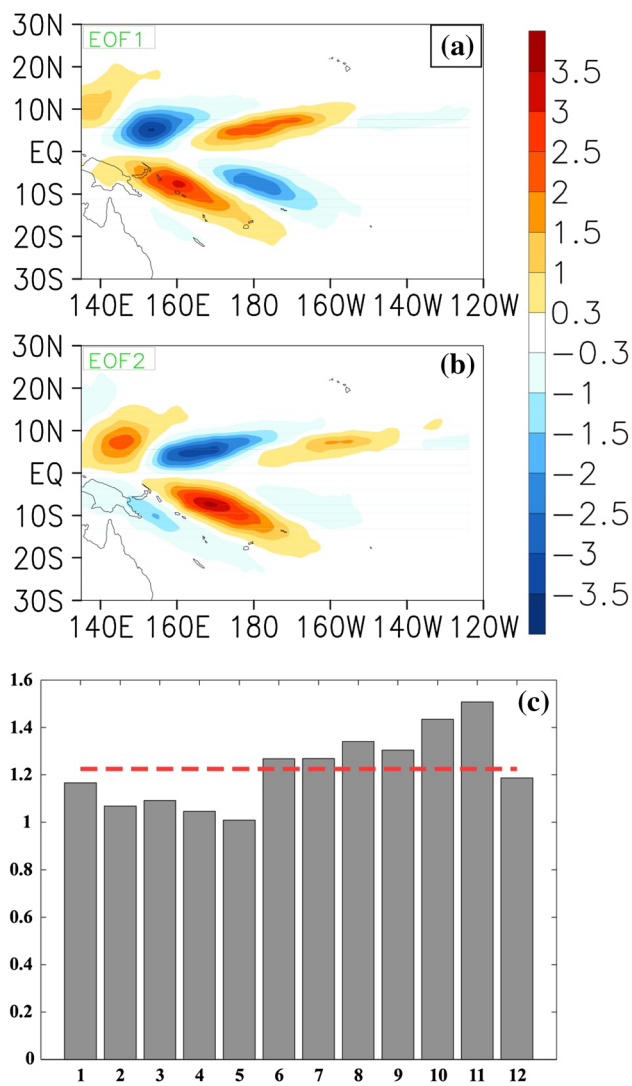
Fig. 8 The first two leading modes, EOF-1 (**a**) and EOF-2 (**b**), for the mixed Rossby-gravity (MRG) wave and the seasonal cycle of the amplitude of the MRG wave with the annual mean amplitude denoted by a red dashed line (**c**)

are maximized at about 7.5°S and 7.5°N. These features are consistent with the geographic distribution and propagation of MRG waves given in previous studies (Wheeler and Kiladis 1999; Dickinson and Molinari 2002; Aiyyer and Molinari 2003). The amplitude of the MRG wave can be computed as $MRG_{amplitude} = \sqrt{PC1^2 + PC2^2}$. In comparison with Figs. 4a and 8c, a consistent seasonal cycle can be found for the wave amplitude of the MRG wave and that of the other four wave types including the MJO, QBWO, ER and SSW.

Figure 9a, b shows the pattern of 2–10-day westward filtered 850-hPa winds and rainfall anomalies regressed onto

the PCs of the first leading MRG wave EOF mode during the days with both active (inactive) MRG waves and SSWs. The active (inactive) MRG or SSW is defined when its amplitude is greater (less) than 1. A clear typical transition of an MRG wave to an SSW wave can be readily found during the days with both active MRG and SSW waves as shown in Fig. 9a. In contrast, such an obvious transition disappears during the days with both inactive MRG and SSW waves (Fig. 9b). Therefore, the days with active (inactive) SSWs and active (inactive) MRG waves are used for characterizing the productivity of the transition of MRG waves to SSW waves. Studies have suggested that TCG could occur when MRG waves transitioned to SSWs (Lau and Lau 1990; Dickinson and Molinari 2002). This transition shown in Fig. 9 partly explains the relatively large fraction of TCG cases attributed to both MRG waves and SSWs. Based upon the ratio of days with active SSW and active MRG waves to the total days for each one given wave phase, the modulation of this transition by the three intra-seasonal wave types (i.e., MJO, QBWO and ER wave) is investigated in the following sections.

A significant impact on this transition by the MJO and ER waves can be clearly observed. During the active MJO phase (e.g., phases 5–6), a higher ratio can be found compared to that during the inactive MJO phase (e.g., phases 2–3) when suppressed convection prevails over the main development region of the WNP basin (Fig. 10a). It is further enhanced by the regression pattern of 850-hPa winds and rainfall anomalies onto the PCs of the first leading MRG wave EOF mode during the active and inactive MJO phases. During the convectively active MJO phase, an apparent equatorial MRG wave propagates from the central Pacific to the western Pacific, and then transits to a well-organized southwest-northeast oriented SSW structure (Fig. 11a). In contrast, such a well-organized SSW train cannot be clearly found during inactive MJO phases 8 and 1–3 (Fig. 11b). Similar modulation of this transition by the ER wave can also be seen. The ratio of days with both active SSW and MRG waves to the total days is largely dependent on the ER phases (Fig. 10c). During ER phases 5–8 when the ER-associated enhanced convection prevails over the southeastern region of the WNP basin, a larger ratio can be readily seen compared to that during the suppressed ER phases 1–4. Correspondingly, a clear southeast-northwest oriented direction SSW can be found along the westward MRG wave (Fig. 11c) during the convectively active ER phases 5–8. When a westward MRG wave coincides with suppressed convection over the southeastern region of the WNP basin during ER phases 1–4, a faint transition of MRG wave to SSW can be observed (Fig. 11d). The transition from MRG to SSW is possibly modulated by the large-scale circulation (such as the monsoon trough), which may further cause changes in

Fig. 9 Regression patterns of 850 hPa-winds and rainfall anomalies on the principal components (PCs) of the first leading MRG wave EOF mode for days with both active SSW and MRG waves (**a**) and with both inactive SSW and MRG waves (**b**). Only values of 850 hPa wind anomalies exceeding the 95% confidence level have been plotted
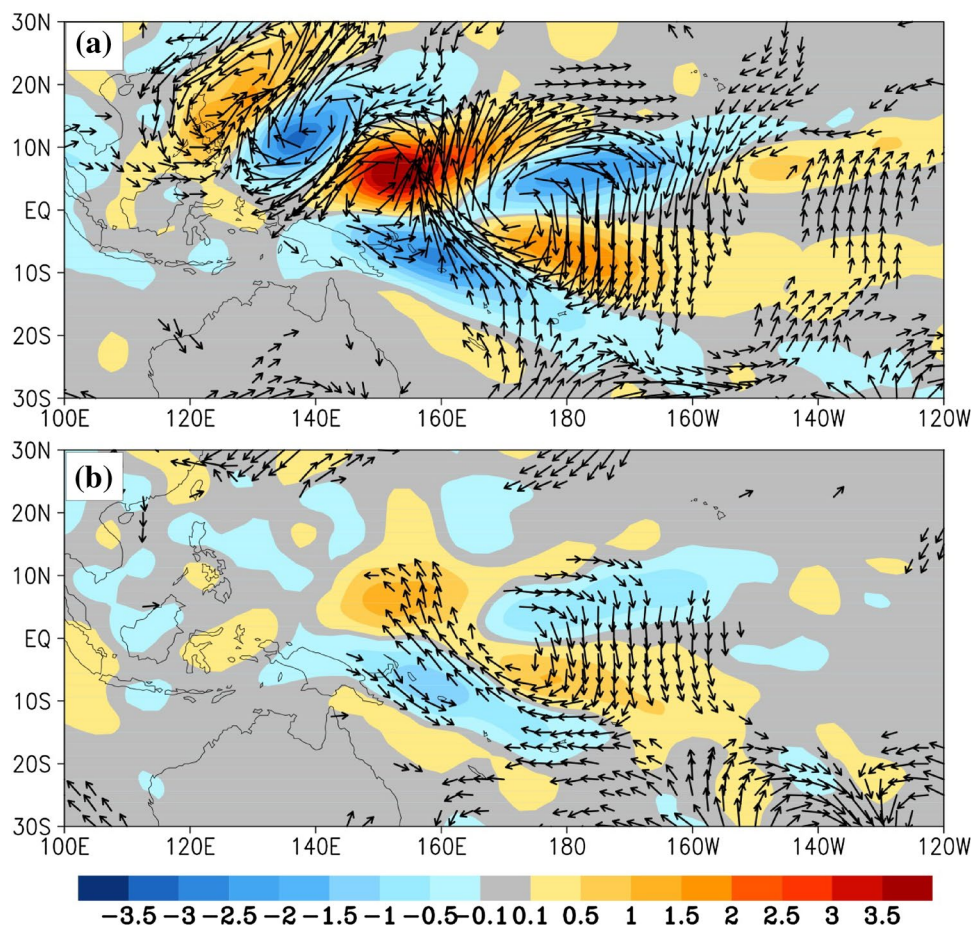
SSW activity (Wu et al. 2015a, b). The MJO and ER may also play a role in this transition. This research topic requires further investigation.

However, no significant difference can be observed in the ratio of days with active SSW and active MRG waves during all QBWO phases (Fig. 10b), which is further confirmed by investigating regression patterns (figure not shown). These results imply that the QBWO plays no substantial role in modulating the transition of MRG waves to SSW waves, which may be closely associated with the northwestward propagation of the QBWO and its local impact. The associated physical causes need further investigation.

6 Summary

It has been recognized that TCG events are closely related to multiple tropical waves (Frank and Roundy 2006; Bessafi and Wheeler 2006, Hsu et al. 2011; Hsu and Li 2011; Schreck et al. 2011, 2012; Chen and Chou 2014). Previous

studies have attributed TCG events over the WNP basin to multiple waves using a TC-centric approach (Schreck et al. 2011; Chen and Chou 2014). However, the local impact of waves tends to be over-emphasized, and the wave-filtered rainfall was likely underestimated by artificially removing TC-related contamination using the TC-centric approach. Moreover, another dominant ISV, the QBWO, which is distinct from the ER wave as shown in this study and previous studies (Zhao and Wu 2018), has a significant modulation on WNP TCG (Chen and Sui 2010; Li and Zhou 2013; Zhao et al. 2015a, b, 2016a, b), The QBWO was not considered in TCG event attribution using the TC-centric approach in previous studies. To overcome these limitations, an approach is proposed based upon EOF analyses for re-assessing the direct association of WNP TCG events with multiple waves. Different from previous studies on the association between multiple waves and TC formation over the WNP basin (Schreck et al. 2011; Chen and Chou 2014; Wu and Takahashi 2007), moreover, our approach used in this study can provide a way for constructing the statistical model based
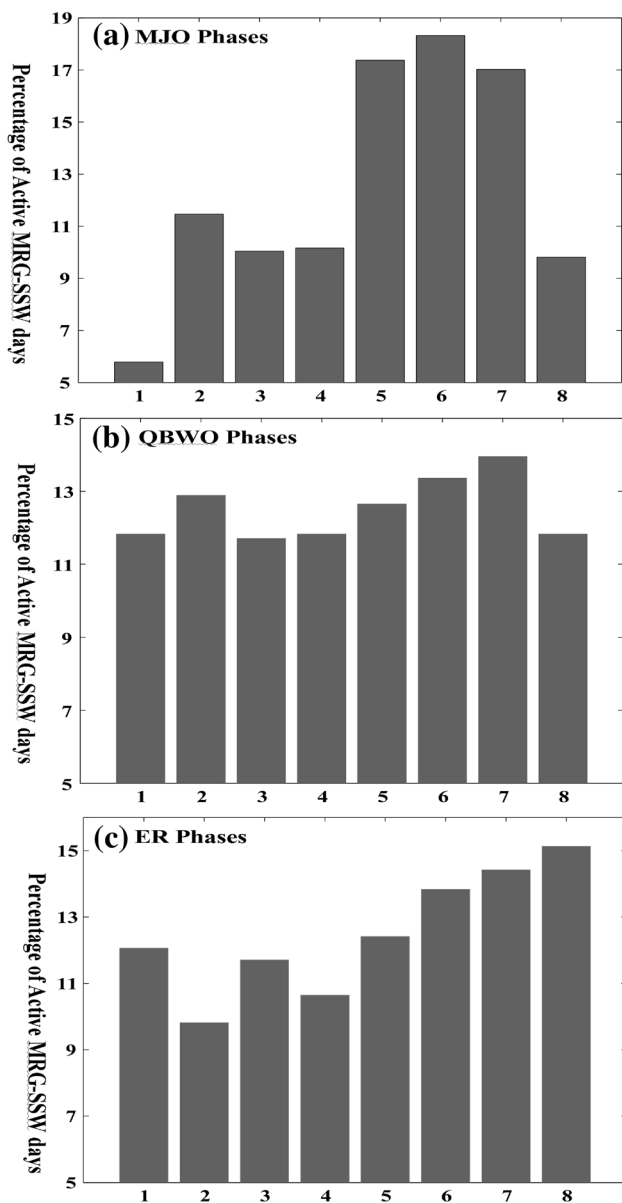
Fig. 10 The ratio (×100) of days with both active SSW and MRG waves to the total days during **a** MJO phases, **b** QBWO phases, and **c** ER phases

upon the temporal coefficients from the first two leading EOFs from these waves for predicting the occurrence of TCs over the WNP basin during weekly periods and daily periods following Vitart et al. (2010) and Leroy and Wheeler (2008). These would be expected in our follow-up study on the construction of statistical models for daily and weekly TC genesis and the associated probabilistic skill.

Results of this study are largely consistent with previous studies (Frank and Roundy 2006; Schreck et al. 2011, 2012;

Chen and Chou 2014). We find that most TCG events are related to more than one wave type, with fewer TCs associated with only a single wave. Only 7 TCs are attributed to a single SSW wave, which is the lowest among the classified four single wave types. That is, without enhancement of dynamic or thermodynamic conditions associated with other large-scale waves, such as the MJO and ER, the amplitude of SSW is not strong enough to cause a significant modulation of TCG events. Moreover, a comparable percentage associated with only the MJO, only the QBWO, and only an ER wave can also be detected, providing possible evidence for some TCG precursors directly from one of these three waves individually on intra-seasonal time scales.

The significant climate modulation of WNP TCG by the MJO and QBWO was well documented in previous studies (Kim et al. 2008; Huang et al. 2011; Zhao et al. 2015a, b, 2016b; Li and Zhou 2013), while the climate modulation of ER waves on WNP TCs has been relatively less studied. In this study, a majority of TCG cases were directly related to the MJO-associated, QBWO-associated and ER-associated categories, accounting for 66, 65 and 68% of the total of 273 WNP TCG cases investigated here, respectively. It indicates that these intra-seasonal waves have a comparably significant association with WNP TCG events. Therefore, the intra-seasonal modulation of WNP TCG by ER waves should be considered in addition to the impact of the MJO and QBWO on TCG. Additionally, about 64% of all of the cases are found to be related to the SSW-associated category, consistent with previous studies that document that SSW trains serve as the majority of precursor disturbances for WNP TCG (Lau and Lau 1990; Holland 1995; Li 2006; Fu et al. 2007).

The modulation of the three intra-seasonal waves on SSW over the WNP basin is further examined by displaying the amplitude and propagation of SSW on intra-seasonal time scales. There is a remarkable modulation of SSW amplitude by MJO and ER waves and evidence of southeast-northwest aligned wave trains, while there is no significant modulation in SSW amplitude by the QBWO or evidence of southeast-northwest aligned wave trains. These modulations of SSW activity by the three wave types may be closely associated with their impact on the transition of the MRG waves to SSW. Results show that the westward MRG waves tend to transit into SSW over the WNP basin during the convectively active phases of the MJO or ER wave compared with their inactive phases. The QBWO does not significantly modulate SSW activity over the WNP or significantly modulate the MRG-SSW transition.
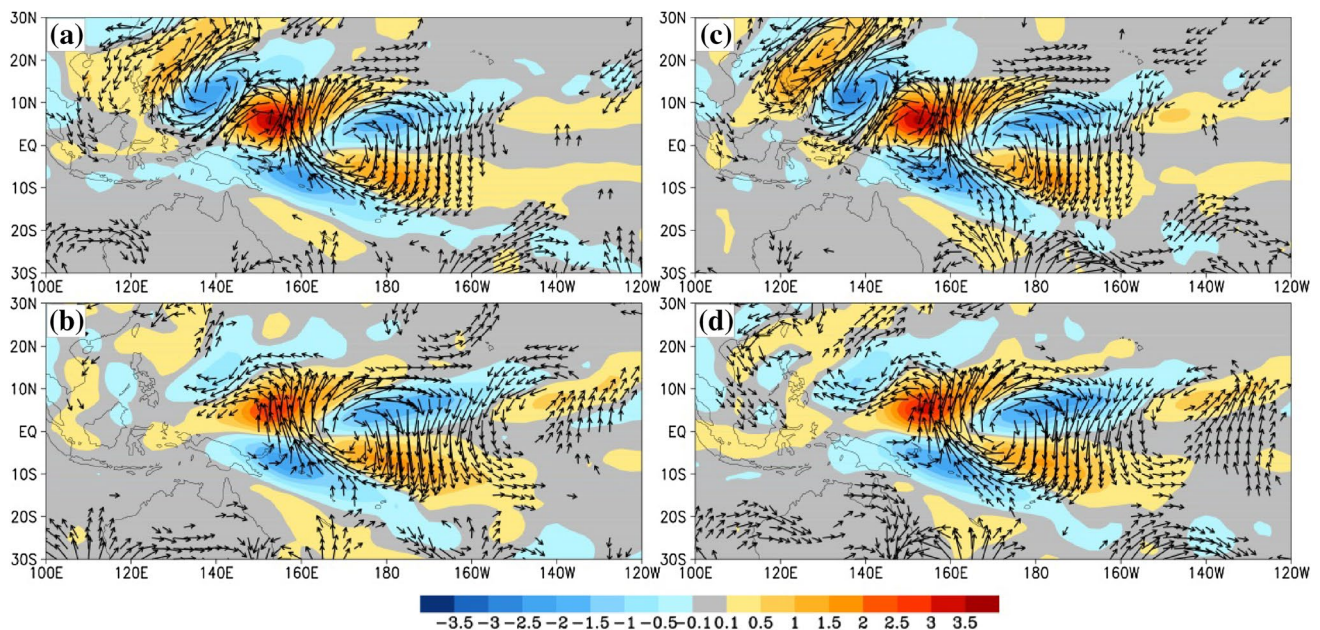
Fig. 11 Regression patterns of 2–10-day westward-filtered rainfall and 850-hPa winds onto the principal components (PCs) of the first leading MRG wave EOF mode during **a** active MJO phases 4–7, **b** inactive MJO phases 8–3, **c** active ER phases 5–8, and **d** inactive ER phases 1–4. Only values of 850 hPa wind anomalies exceeding the 95% confidence level have been plotted

References

Aiyyer A, Molinari J (2003) Evolution of mixed Rossby–gravity waves in idealized MJO environments. J Atmos Sci 65:2837–2855

Bessafi M, Wheeler MC (2006) Modulation of South Indian Ocean tropical cyclones by the Madden–Julian oscillation and convectively coupled equatorial waves. Mon Weather Rev 134:638–656

Bister M, Emanuel KA (1997) The genesis of Hurricane Guillermo: TEXMEX analyses and a modeling study. Mon Weather Rev 125:2662–2682

Camargo SJ, Wheeler MC, Sobel AH (2009) Diagnosis of the MJO modulation of tropical cyclogenesis using an empirical index. J Atmos Sci 66:3061–3074

Chang CP, Chen JM, Harr PA, Carr LE (1996) Northwestward-propagating wave patterns over the tropical western North Pacific during summer. Mon Wea Rev 124:2245–2266

Chen TC, Chen JM (1993) The 10–20-day mode of the 1979 Indian monsoon: its relation with the time variation of monsoon rainfall. Mon Weather Rev 121:2465–2482

Chen G, Chou C (2014) Joint contribution of multiple equatorial waves to tropical cyclogenesis over the western North Pacific. Mon Weather Rev 142:79–92

Chen G, Sui CH (2010) Characteristics and origin of quasi-biweekly oscillation over the western North Pacific during boreal summer. J Geophys Res 115:D14

Dee D et al. (2011) The ERA-Interim reanalysis: configuration and performance of the data assimilation system. Quart J R Meteor Soc 137:553–597

Dickinson M, Molinari J (2002) Mixed Rossby-gravity waves and western Pacific tropical cyclogenesis. Part I: synoptic evolution. J Atmos Sci 59:2183–2196

Dunkerton TJ, Bladwin MP (1995) Observation of 3–6-day meridional wind oscillations over the tropical Pacific, 1973–1992: horizontal structure and propagation. J Atmos Sci 52: 1585–1601. https://doi.org/10.1175/1520-0469(1995)052,1585:OODMWO.2.0.CO;2

Frank WM, Roundy PE (2006) The role of tropical waves in tropical cyclogenesis in the western North Pacific. Mon Weather Rev 134:2397–2417

Fu B, Li T, Peng MS, Weng F (2007) Analysis of tropical cyclogenesis in the western North Pacific for 2000 and 2001. Weather Forecast 22:763–780. https://doi.org/10.1175/WAF1013-1

Gray WM (1968) Global veiw of the origin of tropical disturbances and storms. Mon Wea Rev 96:669–700

Gray WM (1979) Hurricanes: their formation, structure and likely role in the tropical circulation. Meteorology over tropical oceans. Shaw DB (ed), Roy Meteor Soc, James Glaisher House, Grenville Place, Bracknell, Berkshire, RG12 1BX, pp 155–218

Gray WM (1998) The formation of tropical cyclones. Meteor Atmos Phys 67:37–69

Hartmann DL, Maloney ED (2001) The Madden–Julian oscillation, barotropic dynamics, and North Pacific Tropical cyclone formation. Part II: stochastic barotropic modeling. J Atmos Sci 58:2559–2570

Holland GJ (1995) Scale interaction in the western Pacific monsoon. Meteor Atmos Phys 56:57–79

Hsu PC, Li T (2011) Interactions between boreal summer intraseasonal oscillations and synoptic-scale disturbances over the western North Pacific. Part II: apparent heat and moisture sources and eddy momentum transport. J Clim 24:942–961

Hsu HH, Weng CH, Wu CH (2004) Contrasting characteristics between the northward and eastward propagation of the intraseasonal oscillation during the boreal summer. J Clim 17:727–743

Hsu PC, Li T, Tsou CH (2011) Interactions between boreal summer intraseasonal oscillations and synoptic-scale disturbances over the western North Pacific. Part I: energetics diagnosis. J Clim 24:927–941

Huang P, Chou C, Huang RH (2011) Seasonal modulation of tropical intraseasonal oscillations on tropical cyclone geneses in the Western North Pacific. J Clim 24:6339–6352

Huffman GJ, Adler RF, Bolvin DT, Gu G, Nelkin EJ, Bowman KP, Stocker EF, Wolff DB (2007) The TRMM multi-satellite precipitation analysis: Quasi-global, multi-year, combined-sensor precipitation estimates at fine scale. J Hydrometeorol 8:33–55

Jiang X, Li T, Wang B (2004) Structures and mechanisms of the northward propagating Boreal summer intraseasonal oscillation. J Clim 17:1022–1039

Jiang X, Zhao M, Waliser DE (2012) Modulation of tropical cyclones over the Eastern Pacific by the intraseasonal variability simulated in an AGCM. J Clim 25:6524–6538. https://doi.org/10.1175/jcli-d-11-00531-1

Kikuchi K, Wang B (2009) Global perspective of the quasi-biweekly oscillation. J Clim 22:1340–1358

Kim JH, Ho CH, Kim HS (2008) Systematic variation of summertime tropical cyclone activity in the western North Pacific in relation to the Madden–Julian oscillation. J Clim 21:1171–1191

Klotzbach PJ (2010) On the Madden–Julian oscillation–Atlantic hurricane relationship. J Clim 23:282–293

Klotzbach PJ, Oliver ECJ (2015a) Variations in global tropical cyclone activity and the Madden–Julian Oscillation since the mid-twentieth century. Geophys Res Lett 42:4199–4207

Klotzbach PJ, Oliver ECJ (2015b) Modulation of atlantic basin tropical cyclone activity by the Madden–Julian Oscillation (MJO) from 1905 to 2011. J Clim 28:204–217

Klotzbach PJ, Oliver EC, Leeper RD, Schreck CJ III (2016) The relationship between the Madden–Julian Oscillation(MJO) and Southeastern New England Snowfall. Mon Wea Rev 144(4):1355–1362

Kuo HC, Chen JH, Williams RT, Chang CP (2001) Rossby waves in zonally opposing mean flow: behavior in northwest Pacific summer monsoon. J Atmos Sci 58:1035–1050

Kiladis GN, Wheeler MC, Haertel PT, Straub KH, Roundy PE (2009) Convectively coupled equatorial waves. Rev Geophys. https://doi.org/10.1029/2008RG000266

Landsea CW, Bell GD, Gray WM, Goldenberg SB (1998) The extremely active 1995 Atlantic hurricane season: Environmental conditions and verification of seasonal forecasts. Mon Weather Rev 126:1174–1193

Lau KH, Lau NC (1990) Observed structure and propagation characteristics of tropical summertime synoptic-scale disturbances. Mon Weather Rev 118:1888–1913

Lau KH, Lau NC (1992) The energetics and propagation dynamics of tropical summertime synoptic-scale disturbances. Mon Weather Rev 120:2523–2539

Leroy A, Wheeler M (2008) Statistical prediction of weekly tropical cyclone activity in the Southern Hemisphere. Mon Weather Rev 136:3637–3654

Li T (2006) Origin of the summertime synoptic-scale wave train in the western North Pacific. J Atmos Sci 63:1093–1102. https://doi.org/10.1175/JAS3676-1

Li T, Fu B (2006) Tropical cyclogenesis associated with Rossby wave energy dispersion of a pre-existing typhoon. Part I: satellite data analyses. J Atmos Sci 63:1377–1389

Li T, Wang B (1994) The influence of sea surface temperature on the tropical intraseasonal oscillation: a numerical study. Mon Weather Rev 122:2349–2362

Li RCY, Zhou W (2013) Modulation of Western North Pacific tropical cyclone activity by the ISO. Part I: genesis and intensity. J Clim 26:2904–2918

Li T, Ge X, Wang B, Zhu Y (2006) Tropical cyclogenesis associated with Rossby wave energy dispersion of a preexisting typhoon. Part II: numerical simulations. J Atmos Sci 63:1390–1409

Li RCY, Zhou W, Li T (2014) Influences of the Pacific–Japan teleconnection pattern on synoptic-scale variability in the western North Pacific. J Clim 27:140–154. https://doi.org/10.1175/JCLI-D-13-00183.1

Liebmann B, Hendon HH, Glick JD (1994) The relationship between tropical cyclones of the western Pacific and Indian Oceans and the Madden–Julian Oscillation. J Meteorol Soc Jpn 72:401–412

Madden RA, Julian PR (1971) Detection of a 40–50 day oscillation in the zonal wind in the tropical Pacific. J Atmos Sci 28:702–708

Maloney ED, Dickinson MJ (2003) The intraseasonal oscillation and the energetics of summertime tropical western north Pacific synoptic-scale disturbances. J Atmos Sci 60:2153–2168

Molinari J, Knight D, Dickinson M, Vollaro D, Skubis S (1997) Potential vorticity, easterly waves, and eastern Pacific tropical cyclogenesis. Mon Weather Rev 125:2699–2708

Molinari J, Lombardo K, Vollaro D (2007) Tropical cyclogenesis within an equatorial Rossby wave packet. J Atmos Sci 64:1301–1317

Nakazawa T (1986) Intraseasonal variations of OLR in the tropics during the FGGE year. J Meteorol Soc Jpn 64:17–34

Nakazawa T (1988) Tropical super clusters within intraseasonal variations over the Western Pacific. J Meteorol Soc Jpn 66:823–839

North GR, Bell TL, Cahalan RF, Moeng FJ (1982) Sampling errors in the estimation of empirical orthogonal functions. Mon Weather Rev 110:699–706

Reed RJ, Recker EE (1971) Structure and properties of synoptic-scale wave disturbances in the equatorial western Pacific. J Atmos Sci 28:1117–1133

Reed RJ, Norquist DC, Recker EE (1977) The structure and properties of African wave disturbances as observed during phase III of GATE. Mon Weather Rev 105:317–333

Riehl H (1945) Waves in the easterlies and the polar front in the tropics. Univ Chicago Dept Meteorol Misc Rep 17:79 pp

Ritchie EA, Holland GJ (1997) Scale interactions during the formation of typhoon Irving. Mon Weather Rev 125:1377–1396

Ritchie EA, Holland GJ (1999) Large-scale patterns associated with tropical cyclogenesis in the western Pacific. Mon Weather Rev 127:2027–2043

Roundy PE, Frank WM (2004) A climatology of waves in the equatorial region. J Atmos Sci 61:2105–2132

Roundy PE, Schreck CJ (2009) A combined wave-number–frequency and time-extended EOF approach for tracking the progress of modes of large-scale organized tropical convection. Quart J R Meteor Soc 135:161–173

Schreck CJ, Molinari J (2009) A case study of an outbreak of twin tropical cyclones. Mon Weather Rev 137:863–875

Schreck CJ, Molinari J, Mohr KI (2011) Attributing tropical cyclogenesis to equatorial waves in the western North Pacific. J Atmos Sci 68:195–209

Schreck CJ, Molinari J, Aiyyer A (2012) A global view of equatorial waves and tropical cyclogenesis. Mon Weather Rev 140:774–788

Sobel AH, Bretherton CS (1999) Development of synoptic-scale disturbances over summertime tropical Northwest Pacific. J Atmos Sci 56:3106–3127

Sobel AH, Maloney ED (2000) Effect of ENSO and ISO on tropical depressions. Geophys Res Lett 27:1739–1742

Straub KH, Kiladis GN (2003) Interactions between the boreal summer intraseasonal oscillation and higher-frequency tropical wave activity. Mon Weather Rev 131:945–960

Takayabu Y, Nitta T (1993) 3–5 day period disturbances coupled with convection over the tropical Pacific Ocean. J Meteorol Soc Jpn 71:221–246

Tam CY, Li T (2006) Origin and dispersion characteristics of the observed tropical summertime synoptic scale waves over the western Pacific. Mon Weather Rev 134:1630–1646

Vitart F, Leroy A, Wheeler MC (2010) A comparison of dynamical and statistical predictions of weekly tropical cyclone activity in the southern hemisphere. Mon Weather Rev 138:3671–3682. https://doi.org/10.1175/2010mwr3343.1

Wallace JM, Chang CP (1969) Spectral analysis of large-scale wave disturbances in the lower tropical troposphere. J Atmos Sci 26:1010–1025

Wang B, Rui H (1990) Synoptic climatology of transient tropical intraseasonal convection anomalies: 1975–1985. Meteorol Atmos Phys 44(1–4):43–61

Wang B, Xie X (1996) Low-frequency equatorial waves in vertically sheared zonal flow. Part I: stable waves. J Atmos Sci 53:449–467

Wang B, Xie X (1997) A model for the boreal summer intraseasonal oscillation. J Atmos Sci 54:72–86

Wheeler MC, Hendon HH (2004) An all-season real-time multivariate MJO index: development of an index for monitoring and prediction. Mon Weather Rev 132:1917–1932

Wheeler M, Kiladis GN, Webster PJ (2000) Large-scale dynamical fields associated with convectively coupled equatorial waves. J Atmos Sci 57:613–640

Wu L, Takahashi M (2017) Contributions of tropical waves to tropical cyclone genesis over the western North Pacific. Clim Dyn. https://doi.org/10.1007/s00382-00017-03895-00383

Wu L, Wen Z, Li T, Huang R (2014) ENSO-phase dependent TD and MRG wave activity in the western North Pacific. Clim Dyn 42:1217–1227

Wu L, Wen Z, Wu R (2015a) The monsoon trough and the evolution of westward-propagating tropical waves in the western North Pacific. Part I: observations. J Clim 28:7108–7127

Wu L, Wen Z, Wu R (2015b) The monsoon trough and the evolution of westward-propagating tropical waves in the western North Pacific. Part II: energetics and numerical experiments. J Clim 28:9332–9349

Yang GY, Hoskins B, Slingo J (2007) Convectively coupled equatorial waves. Part II: synthesis structures and their forcing and evolution. J Atmos Sci 64:3438–3451

Yasunari T (1979) Cloudiness fluctuations associated with the northern hemisphere summer monsoon. J Meteorol Soc Japan 57:227–242

Zehr RM (1992) Tropical cyclogenesis in the western north Pacific. NOAA Tech Rep NESDIS 61:181

Zhao H, Wu L (2018) Modulation of convectively coupled equatorial Rossby wave on the Western North Pacific tropical cyclones activity. Int J Climatol 38(2):932–948. https://doi.org/10.1002/joc-5220

Zhao H, Jiang X, Wu L (2015a) Modulation of Northwest pacific tropical cyclone genesis by the intraseasonal variability. J Meteorol Soc Jpn 93:1. https://doi.org/10.2151/jmsj-2015-006

Zhao H, Yoshida R, Raga GB (2015b) Impact of the Madden–Julian oscillation on western north Pacific tropical cyclogenesis associated with large-scale patterns. J Appl Meteorol Climatol 54:413–1429

Zhao H, Jiang X, Wu L (2016a) Boreal summer synoptic-scale waves over the Western North Pacific in multi-model simulations. J Clim 29:4487–4508

Zhao H, Wang C, Yoshida R (2016b) Modulation of tropical cyclogenesis in the western North Pacific by the quasi-biweekly oscillation. Adv Atmos Sci 33(12):1361–1375

Zhao H, Raga GB, Klotzbach PJ (2018) Impact of the boreal summer quasi-biweekly oscillation on Eastern North Pacific tropical cyclone activity. Int J Climatol 38(3):1353–1365

Zhou X, Wang B (2007) Transition from an eastern Pacific upper-level mixed Rossby-gravity wave to a west Pacific tropical cyclone. Geophys Res Lett 34:L24801